AD-A111 401 DEFENSE MAPPING AGENCY AEROSPACE CENTER ST LOUIS AFS MO F/G 8/2
MATRIX DATA ANALYSIS: COLOR/B&W CODING IS NOT ALWAYS ENOUGH.(U)
1981 M B FAINTICH, G B SIGLER, J D SIMPSON

UNCLASSIFIED NL

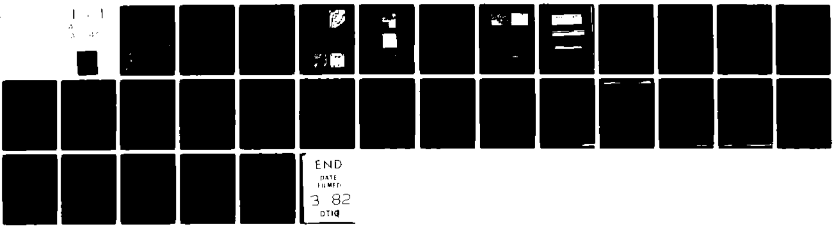

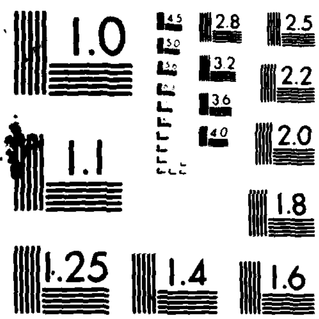

MICROCOPY RESOLUTION TEST CHART
NATIONAL BUREAU OF STANDARDS 1963 A

ADA111401

UNCLASSIFIED

SECURITY CLASSIFICATION OF THIS PAGE (When Data Entered)

REPORT DOCUMENTATION PAGE

READ INSTRUCTIONS BEFORE COMPLETING FORM

1. REPORT NUMBER

2. GOVT ACCESSION NO. AD-A111 401

3. RECIPIENT'S CATALOG NUMBER

4. TITLE (and Subtitle)
Matrix Data Analysis: Color/B&W Coding is Not Always Enough

5. TYPE OF REPORT & PERIOD COVERED
Interim, 1976-1981

6. PERFORMING ORG. REPORT NUMBER
N/A

7. AUTHOR(s)
Dr. Marshall B. Faintich
Mr. George B. Sigler
Mr. James D. Simpson

8. CONTRACT OR GRANT NUMBER(s)
N/A

9. PERFORMING ORGANIZATION NAME AND ADDRESS
Defense Mapping Agency Aerospace Center
St. Louis AFS, MO 63118

10. PROGRAM ELEMENT, PROJECT, TASK AREA & WORK UNIT NUMBERS
N/A

11. CONTROLLING OFFICE NAME AND ADDRESS
Defense Mapping Agency

12. REPORT DATE
~~N/A~~ 1981

13. NUMBER OF PAGES
29

14. MONITORING AGENCY NAME & ADDRESS (if different from Controlling Office)

15. SECURITY CLASS. (of this report)
Unclassified

15a. DECLASSIFICATION/DOWNGRADING SCHEDULE

16. DISTRIBUTION STATEMENT (of this Report)
Unlimited.

This document has been approved for public release and sale; its distribution is unlimited.

DTIC ELECTE FEB 26 1982 A

17. DISTRIBUTION STATEMENT (of the abstract entered in Block 20, if different from Report)

18. SUPPLEMENTARY NOTES
To be presented at the Inter-Congress Symposium, International Society of Photogrammetry and Remote Sensing Commission III, Otaniemi, Finland, 7-11 June 1982.

19. KEY WORDS (Continue on reverse side if necessary and identify by block number)
Image Displays, Data Bases, Matrix Analysis

20. ABSTRACT (Continue on reverse side if necessary and identify by block number)
The Defense Mapping Agency produces digital cartographic data bases that describe the physical appearance of the surface of the earth. Specialized processing and display techniques such as convolution filtering, texture discrimination, and specialized color/B&W displays allow for sophisticated analyses that are applicable to all types of matrix data.

DD FORM 1 JAN 73 1473 EDITION OF 1 NOV 65 IS OBSOLETE

Unclassified

SECURITY CLASSIFICATION OF THIS PAGE (When Data Entered)

DTIC FILE COPY

MATRIX DATA ANALYSIS: COLOR/B&W CODING IS NOT ALWAYS ENOUGH

Dr. Marshall B. Faintich
Chief, Aerospace Cartography Department Techniques Office
George B. Sigler
Advanced Systems Branch, Directorate of Plans & Requirements
James D. Simpson
Scientific Data Department, Techniques Office
Defense Mapping Agency Aerospace Center
St. Louis Air Force Station, Missouri 63118

ABSTRACT

The Defense Mapping Agency produces digital cartographic data bases that describe the physical appearance of the surface of the earth. Specialized processing and display techniques such as convolution filtering, texture discrimination, and specialized color/B&W displays allow for sophisticated analyses that are applicable to all types of matrix data.

MATRIX DATA ANALYSIS
COLOR/B&W CODING IS NOT ALWAYS ENOUGH

Background

The Defense Mapping Agency produces digital data bases that describe the physical appearance of the surface of the earth. These data bases include, but are not limited to, terrain elevation, culture including landscape characteristics, and vertical features. This data is collected from digitized source maps, from optically or digitally correlated stereo-pairs of photographic imagery, and from digital multi-spectral sensor data. A dramatic impact has been made in the ability to analyze these digital data bases by applying state-of-the-art digital image technology processing and display concepts. These include a variety of color and/or black and white displays of not only intensity/color coded matrix data, but also image processed data using specialized convolution filters, texture discrimination, and special color representation techniques. In addition, computer generated imagery from these data bases serves as a final analysis tool.

Techniques and Results

With results similar to those from manually compiled classical mapping and charting displays, digital terrain elevation data may be used to generate a standard contour plot (figure 1.) and the corresponding tint plate (figure 2.) in which the areas between contour lines are either color or gray level coded. An alternative is to color or gray level code the matrix terrain data directly. While analysis of these matrix image displays is superior to trying to perform analysis by visual inspection of the data in printed numerical matrix format, they only provide for a low spatial resolution analysis capability. Shaded relief display with variable illumination adds additional information for analysis of all types of matrix data, but is particularly meaningful for cartographic data because of the relationship to the physical world. Higher spatial resolution analysis of the shaded relief display may be gained by applying photogrammetric models to generate pseudo-stereo-pairs of images (figure 3.) in which spike points are apparent under stereoscopic analysis. These techniques, used singly or in combination, allow for matrix data analysis far superior to techniques of a decade ago, but they are not enough.

In order to perform high resolution anomaly analysis of matrix data for the purpose of either quality control or information gathering, advanced techniques are required. These techniques include convolution filtering, texture discrimination, and specialized color representation. [illegible] about the algorithms used in these techniques are described in Appendices [illegible] through E.

Convolution filters have been used very effectively to enhance matrix data to show processing anomalies as well as where data has been merged from different production equipment, different stereo models, different production methods, variable requirement specifications, and even from different analysts. These types of filters are used extensively by the image processing community to detect edge differences, and then to re-apply the differences to sharpen the original image. They also have been shown to be a powerful tool for the analysis of matrix data. Consider figures 4a. and 4b. Depicted are a shaded relief display and the corresponding digital convolution display of a one degree square of digital

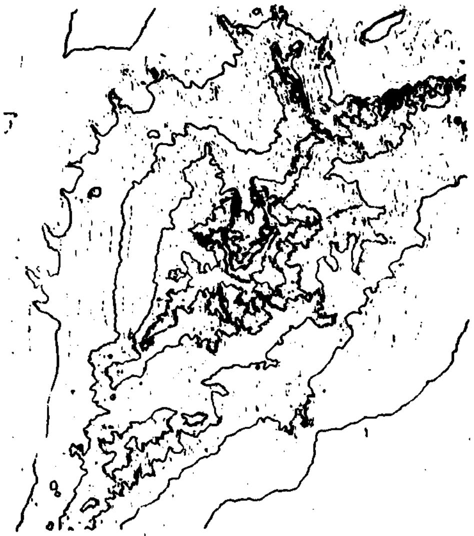

FIGURE 1. CONTOURS GENERATED FROM DIGITAL TERRAIN DATA

FIGURE 2. GREY LEVEL CODED ELEVATION TINT PLATE

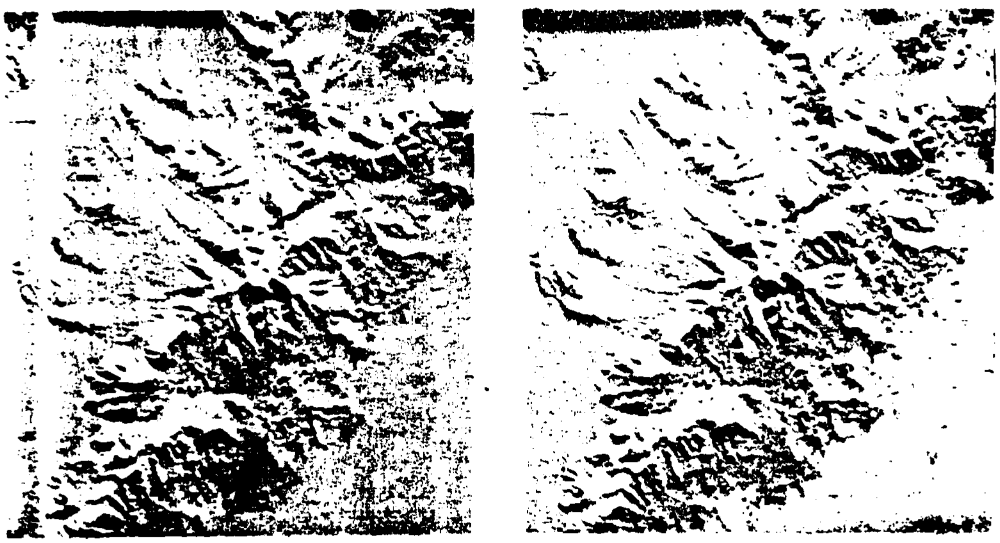

FIGURE 3. COMPUTER GENERATED STEREO-PAIR

FIGURE 4a. SHADED RELIEF OF TERRAIN DATA

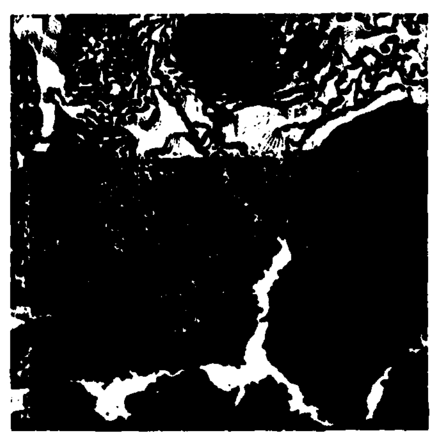

FIGURE 4b. CONVOLUTION MASK RESULTS OF TERRAIN DATA

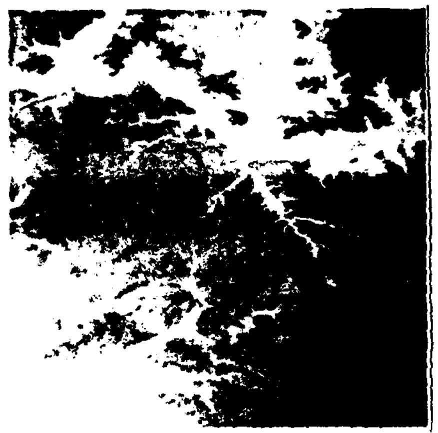

FIGURE 5a. GRAY LEVEL CODED ELEVATION DISPLAY

FIGURE 5b. SHADED RELIEF DISPLAY

FIGURE 5c. CONVOLUTION DISPLAY

terrain elevation data produced from both digitized source maps and stereo-pairs of imagery. The shaded relief display, as well as the corresponding gray level coded elevation display, does not clearly suggest that the data was produced by two methods. In contrast, the convolution display clearly delineates the difference. In the top third of the display, the contouring effect due to interpolation of digitized source maps is clearly visible, and is starkly contrasted with the rest of the display, wherein stereoplotter noise plus real high frequency data combine to produce a variety of edge differences.

Texture analysis has proven to be very powerful for discriminating small area data that has been merged into larger matrices. For example, digital elevation data produced at a one arc second interval was sampled and merged with three arc second data. This data merge is not apparent in the gray level coded elevation display (figure 5a.). Because of inherent higher frequency information in the one arc second data, there is a noticeable difference between the textures of the levels of data in the shaded relief display, and an even more apparent difference in the convolution display (see figures 5b., 5c.). A similar difference is noticed when high frequency digital culture data is merged with lower resolution data.

For the purpose of determining compatability between data types, such as between digital terrain and culture data, simple color coding and overlay in Red-Green-Blue (RGB) space may not be sufficient. A more powerful technique employs coding each data type along an Intensity-Hue-Saturation (IHS) axis and then converting from IHS space to RGB space prior to display. Since the visual perception process can distinguish variation between IHS, the data types can be overlayed without a merging of colors, and therefore, without an information loss. Consider figures 6a.-6e. Figures 6a. and 6b. are gray level displays of terrain shaded relief and digital culture information, respectively. These two matrices were assigned as Intensity and Hue, respectively, with Saturation held constant. Figures 6c.-6e. are the Red, Green, and Blue components of the final IHS color-coded image.

Finally, and probably unique to map type data, is the technique of computer generating landform scenes as seen by various visual and electro-optical sensors. This allows for a final quality control analysis of information content, and also has been very valuable in the definition of data base requirement specification. Figures 7a.-7c. depict computer generated visual simulations and actual photography over the data base shown in the IHS figures.

<u>Impact</u>

The impact of these digital image technology concepts to matrix data display and analysis has been enormous. Not only has there been a greatly increased capability for the degree and sophistication of quality control, but there is an associated cost savings in both the quality control review process, and in the resultant expense of using matrix data containing anomalies. These techniques have application to all types of matrix data production as well as for the analysis of all types of real matrix data.

FIGURE 6a. INTENSITY COMPONENT: SHADED RELIEF DATA

FIGURE 6b. HUE COMPONENT: DIGITAL CULTURE DATA

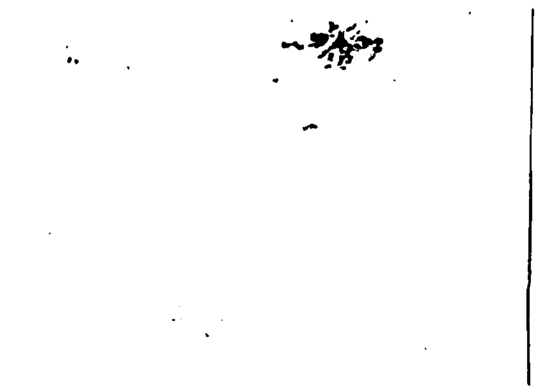

FIGURE 6c. RED COMPONENT

FIGURE 6d. GREEN COMPONENT

FIGURE 6e. BLUE COMPONENT

FIGURES 6a-6e. INTENSITY AND HUE INPUT DATA TRANSFORMED TO RED, GREEN, AND BLUE OUTPUT DATA.

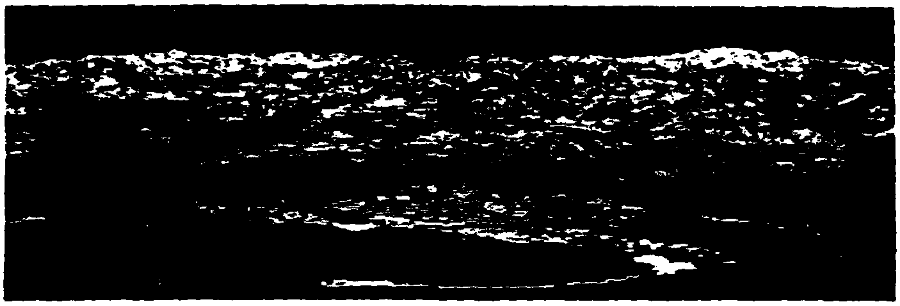

FIGURE 7a. **Visual Simulation from 10,000 foot Altitude**

FIGURE 7b. **Visual Simulation from Shipboard Level**

FIGURE 7c. **Actual Photograph from Shipboard Level**

Figures 7a-7c Port Angeles, Washington and Mt. Olympus: Comparison Between Visual Simulations and Actual Photography

Acknowledgement

Along with the authors, the following individuals contributed to the development of results presented in this paper: Dr. Richard Berg, Mr. John Gough, Mr. Thomas Sellers, and Mr. Paul Pals.

References

Buchanan, M. D.; 1979; "Effective Utilization of Color in Multidimensional Data Presentations," SPIE Proceedings, Volume 199, pp. 9-18.

Faintich, M.; Sigler, G.; Fahy, D.; 1978; "Advances in Digital Image Display and Simulation from Digital Terrain Data Bases," Proceedings of the International Society of Photogrammetry Symposium, Commission IV, Ottawa, Canada, 2-6 October 1978, pp. 111-135 (reprinted in The Optronics Journal, May 1979, pp. 1, 4-7).

Faintich, M. B.; 1979; "Digital Image Technology: MC&G Impact," Harvard Library of Computer Graphics/1980 Mapping Collection," Volume 10, pp. 29-40. (Reprinted in condensed form in the Proceedings of the American Society of Photogrammetry: 1980 Annual Convention, pp. 32-43.)

Faintich, M. B.; 1981; "Digital Cartographic Systems at the Defense Mapping Agency Aerospace Center," SPIE Proceedings, Volume 301, paper 301-25.

Appendix A. Elevation Image Algorithm

Digital terrain elevation data (DTED) consists of terrain elevation values, in integer meters, stored on tape in matrix format. The DTED is organized into one-degree by one-degree square geographic areas with a maximum of ten one-degree squares on any one tape. For a given area of interest, not necessarily a one-degree square, consider the DTED values to form an p by q matrix, T. The first row of such a T matrix, as well as all other p by q matrices described here and in other sections, corresponds geographically to the southernmost values represented by the matrix. Consequently, in the schematic for a T matrix, as presented in Figure A.1, the row convention is correct even though it appears to be an inversion of the customary method of displaying matrix rows.

$$T = \begin{bmatrix} t_{p,1} & t_{p,2} & \cdots\cdots\cdots & t_{p,q} \\ \cdots & \cdots & \cdots\cdots\cdots & \cdots \\ \cdots & \cdots & \cdots\cdots\cdots & \cdots \\ \cdots & \cdots & \cdots\cdots\cdots & \cdots \\ t_{2,1} & t_{2,2} & \cdots\cdots\cdots & t_{2,q} \\ t_{1,1} & t_{1,2} & \cdots\cdots\cdots & t_{1,q} \end{bmatrix}$$

Figure A.1 Schematic for a T Matrix

Let $t_{i,j}$ denote the DTED value in the ith row and jth column of T. Similarly, let $e_{i,j}$ denote the corresponding pixel in an p by q matrix, E, which is to be recorded on film as a digital image display of T as a gray level coded elevation image. A gray level value for each pixel of E may be determined by the simple scaling algorithm below.

1. Compute a gray level value for $e_{i,j}$ by

$$e_{i,j} = \text{integer} \left[\left(\frac{t_{i,j} - t_{min}}{t_{max} - t_{min}} \right) \cdot (G_{max} - G_{min}) \right] \qquad \text{(A.1)}$$

where:

$t_{i,j}$ = DTED value in the ith row and jth column of T

t_{min} = minimum DTED value in T

t_{max} = maximum DTED value in T

G_{max} = maximum gray level value allowed in E, usually 255

G_{min} = minimum gray level value allowed in E, usually 0

$i = 1,2,\ldots,p$

$j = 1,2,\ldots,q$

2. Constrain the $e_{i,j}$ from equation (A.1) to be in the interval (G_{min}, G_{max}). That is, set

$$e_{i,j} = \begin{Bmatrix} G_{min} \\ G_{max} \end{Bmatrix} \quad \text{if} \quad \begin{Bmatrix} e_{i,j} \leq G_{min} \\ e_{i,j} > G_{max} \end{Bmatrix} \tag{A.2}$$

where:

G_{min} = minimum gray level value allowed in E, usually 0

G_{max} = maximum gray level value allowed in E, usually 255

$i = 1,2,\ldots,p$

$j = 1,2,\ldots,q$

Note the constraints of equation (A.2) are imposed along with a G_{min} value of zero to change any $e_{i,j}$ having a computed value, on a UNIVAC 1100 series computer, of minus zero (36-bit word of ones) to a positive zero (36-bit word of zeros). Further, this change in $e_{i,j}$ zero representation must be performed before the right-most 8-bit byte of each $e_{i,j}$ is extracted and recorded on tape as an output pixel, because extracting the right-most byte from an $e_{i,j}$ value of minus zero would incorrectly yield an output pixel gray level value of 255 (8-bit byte of ones). A similar rationale is the motivation for the constraints imposed by equations (B.3) and (C.6) of Appendices B and C, respectively.

Appendix B. Relief Image Algorithm

Let $r_{i,j}$ denote the gray level value in the ith row and jth column of an p by q matrix, R, of shaded relief pixels over the geographic area represented by T (see Appendix A). The algorithm below may be used to compute any $r_{i,j}$ provided T is available and assuming the area depicted by R is illuminated from the Northwest.

1. Compute the elevation difference, ΔEL, between $t_{i,j}$ and it's neighbor $t_{i-1,j+1}$, by

$$\Delta EL = t_{i,j} - t_{i-1,j+1} \tag{B.1}$$

where:

$t_{i,j}$ = DTED value in the ith row and jth column of T

$t_{i-1,j+1}$ = DTED value in the (i-1)th row and (j+1)th column of T

$i = 2,3,\ldots, p-1$

$j = 2,3,\ldots, q-1$

2. Compute a gray level value for each $r_{i,j}$ from

$$r_{i,j} = \text{integer}\left[\frac{\Delta EL \cdot \lambda_r + (1)\cdot \text{sign}(\Delta EL)\cdot f}{\Delta g_{min}}\right]\cdot(\Delta g_{min}) + b \qquad \text{(B.2)}$$

where:

ΔEL = elevation difference, in integer meters, from equation (B.1)

λ_r = multiplicative scale factor, computed as $(G_{max} - G_{min} + 1)/\left[2 \cdot \exp(\Delta EL_{max})\right]$

G_{max} = integer value for maximum gray level value allowed in R, usually 255

G_{min} = integer value for minimum gray level value allowed in R, usually 0

$\exp(\Delta EL_{max})$ = maximum expected elevation difference, either an arbitrary constant or computed as $\text{integer}\left[4 \cdot \exp(\sigma_{\Delta EL}) + .99\right]$

$\exp(\sigma_{\Delta EL})$ = (1%) $(t_{max} - t_{min})$. Note this expression for $\exp(\sigma_{\Delta EL})$ is the result of a least square line fit to the actual $\sigma_{\Delta EL}$ values for ~~the~~ various DTED examples, studied ~~presented in an earlier section. Further studies may modify this expression.~~

t_{max} = maximum DTED value in T

t_{min} = minimum DTED value in T

Δg_{min} = minimum gray level step, computed as the integer value of $(G_{max} - G_{min} + 1)/(N_g - 1)$

N_g = integer number of unique gray levels allowed in R, usually 33

f = round off factor, computed as $(\Delta g_{min} - \lambda_r)$, but set to zero if the computed value is negative

b = bias term used to assign a background gray level value to any $r_{i,j}$ in a region of relatively constant height, computed as the integer value of $(G_{max} - G_{min})/2$

i = 2,3,..., p-1

j = 2,3,..., q-1

3. Constrain the $r_{i,j}$ from equation (B.2) to be in the interval (G_{min}, G_{max}). That is, set

$$r_{i,j} = \begin{Bmatrix} G_{min} \\ G_{max} \end{Bmatrix} \quad \text{if} \quad \begin{Bmatrix} r_{i,j} \le G_{min} \\ r_{i,j} > G_{max} \end{Bmatrix} \tag{B.3}$$

where:

G_{max} = maximum gray level value allowed in R, usually 255

G_{min} = minimum gray level value allowed in R, usually 0

$i = 2,3,\ldots, p-1$

$j = 2,3,\ldots, q-1$

After the $r_{i,j}$ have been determined by equation (B.3), R may be completed by setting all elements in rows 1 and p and columns 1 and q to zero (clear).

Appendix C. Convolution Image Algorithm

Again, as discussed in Appendix A, consider the DTED values to form an p by q matrix, T, where $t_{i,j}$ denotes the DTED value in the $i\underline{th}$ row and $j\underline{th}$ column of T. Similarly, let $c_{i,j}$ denote the corresponding pixel in an p by q matrix, C, which is to be recorded on film as a digital image. Let H, an ℓ by ℓ matrix, denote a filter to be applied to T via a discrete convolution process. Matrix C is produced by convolving T with H and subsequently applying a noise-cleaning and gray level mapping process. Individual elements of C may be determined by the algorithm below.

1. Form an p by q matrix, T', of elevation differences relative to the minimum DTED value, t_{min}, in T via

$$t'_{i,j} = t_{i,j} - t_{min} \tag{C.1}$$

where:

$t_{i,j}$ = DTED value in the $i\underline{th}$ row and $j\underline{th}$ column of T

t_{min} = minimum DTED value in T

$i = 1,2,...,p$

$j = 1,2,...,q$

2. Convolve T' with H to produce an p by q matrix, V, by

$$v_{i,j} = \sum_{m=1}^{\ell} \sum_{n=1}^{\ell} \left(t'_{m+i-\frac{\ell+1}{2},\, n+j-\frac{\ell+1}{2}}\right) \cdot \left(h_{m,n}\right) \tag{C.2}$$

where:

$t'_{m+i-\frac{\ell+1}{2},\, n+j-\frac{\ell+1}{2}}$ = elements of elevation difference matrix, T', from equation (C.1)

$h_{m,n}$ = elements of filtering matrix, e.g., one of those listed in Appendix D

ℓ = an odd integer indicating the row and column dimensions of H, usually 3

$i = \frac{\ell+1}{2}, \frac{\ell+1}{2} + 1, \frac{\ell+1}{2} + 2, \ldots, p - \frac{\ell-1}{2}$

$j = \frac{\ell+1}{2}, \frac{\ell+1}{2} + 1, \frac{\ell+1}{2} + 2, \ldots, q - \frac{\ell-1}{2}$

After the $v_{i,j}$ have been determined by equation (C.2), V may be completed by setting all elements in the outer rows, i.e., $i = 1, \ldots, \frac{\ell-1}{2}$ $i = p - \frac{\ell-1}{2}, \ldots, p$ and outer columns, i.e., $j = 1, \ldots, \frac{\ell-1}{2}$ $j = q - \frac{\ell-1}{2}, \ldots, q$ to zero. Note the total number, N_o, of elements in the perimeter region of V set to zero by this process ~~are~~ is depicted as the hachured portion of Figure C.1 and may be computed via

$$N_o = (\ell - 1) \cdot \left[(p + q) - (\ell - 1)\right] \tag{C.3}$$

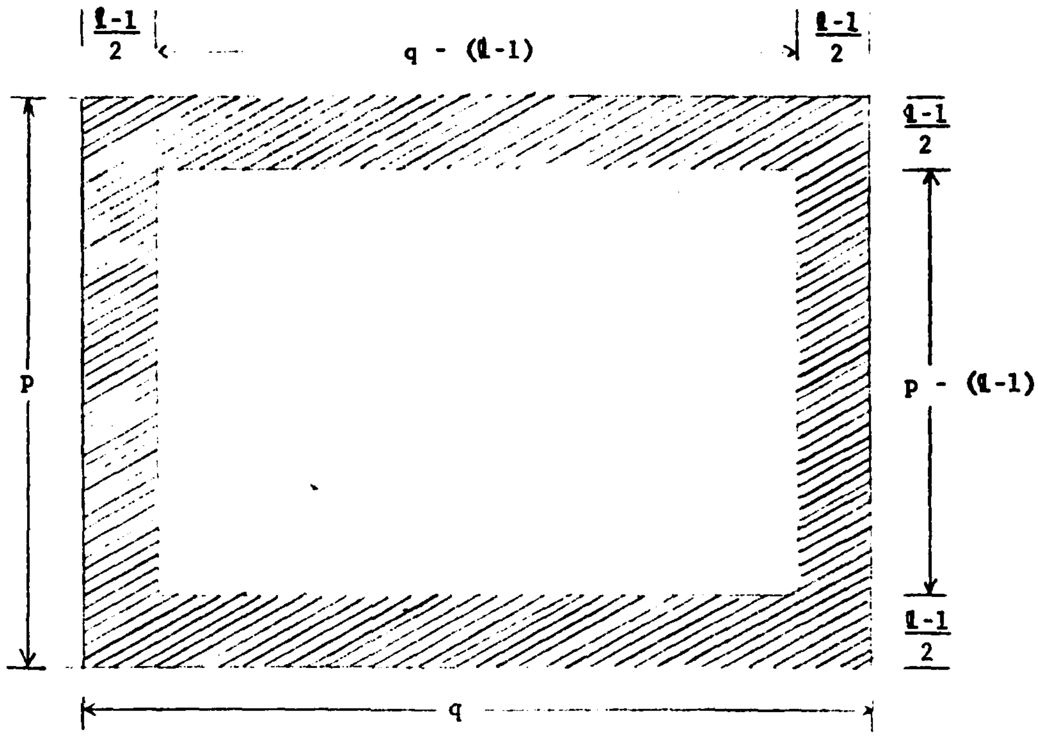

Figure C.1 Schematic of Zeroed Elements in Matrix V

3. Apply a noise-cleaning process to V to produce an p by q matrix, W, via

$$w_{i,j} = \text{integer}\left|\frac{v_{i,j} + (1)\cdot[\text{sign}\,(v_{i,j})]\cdot\left|\frac{h_{mid}}{2}\right|}{\left|h_{mid}\right|}\right| \tag{C.4}$$

where:

$|\;|$ = indicates absolute value

$v_{i,j}$ = elements of convolution matrix, V, from equation (C.2)

h_{mid} = center term of filter matrix, H, i.e., $h_{\frac{l+1}{2},\frac{l+1}{2}}$

$i = 1,2, \ldots, p$

$j = 1,2, \ldots, q$

4. Compute elements of matrix C by gray level mapping W according to

$$c_{i,j} = w_{i,j} \cdot \lambda_c + b \tag{C.5}$$

where:

$w_{i,j}$ = elements of W, from equation (C.4)

b = bias term, usually 20

λ_c = gray level mapping scale factor, usually 8

$i = 1,2, \ldots, p$

$j = 1,2, \ldots, q$

5. Constrain the $c_{i,j}$ from equation (C.5) to be in the interval (G_{min}, G_{max}).

That is, set

$$c_{i,j} = \begin{Bmatrix} G_{min} \\ G_{max} \end{Bmatrix} \quad \text{if} \quad \begin{Bmatrix} c_{i,j} \leq \epsilon \\ c_{i,j} > G_{max} \end{Bmatrix} \tag{C.6}$$

where:

G_{min} = minimum gray level value allowed in C, usually 0

G_{max} = maximum gray level value allowed in C, usually 255

ϵ = threshold value chosen to force output gray level values of G_{min} for those $c_{i,j}$ in a region of DTED values of relatively constant height, usually 21

$i = 1,2, \ldots, p$

$j = 1,2, \ldots, q$

Appendix D. Convolution Masks

Twenty-seven masks were selected for testing and built into a computer program, DMATER, used to generate test images via these filters. The first three are Laplacian edge detection masks while the remaining twenty-four masks allow for computing 1st through 6th differences in the N-S, E-W, NW-SE, and SW-NE directions. Specific matrix elements for each mask along with a unique reference number, in parenthesis, to its left are provided below.

The three Laplacian masks are:

$$(1)\quad \begin{matrix} 0 & -1 & 0 \\ -1 & 4 & -1 \\ 0 & -1 & 0 \end{matrix}$$

$$(2)\quad \begin{matrix} -1 & -1 & -1 \\ -1 & 8 & -1 \\ -1 & -1 & -1 \end{matrix}$$

$$(3)\quad \begin{matrix} 1 & -2 & 1 \\ -2 & 4 & -2 \\ 1 & -2 & 1 \end{matrix}$$

The masks for 1st through 6th differences in the N-S direction are:

$$(4)\quad \begin{matrix} 0 & -1 & 0 \\ 0 & 1 & 0 \\ 0 & 0 & 0 \end{matrix}$$

$$(5)\quad \begin{matrix} 0 & 1 & 0 \\ 0 & -2 & 0 \\ 0 & 1 & 0 \end{matrix}$$

$$(6)\quad \begin{matrix} 0 & 0 & -1 & 0 & 0 \\ 0 & 0 & 3 & 0 & 0 \\ 0 & 0 & -3 & 0 & 0 \\ 0 & 0 & 1 & 0 & 0 \\ 0 & 0 & 0 & 0 & 0 \end{matrix}$$

$$(7)\quad \begin{matrix} 0 & 0 & 1 & 0 & 0 \\ 0 & 0 & -4 & 0 & 0 \\ 0 & 0 & 6 & 0 & 0 \\ 0 & 0 & -4 & 0 & 0 \\ 0 & 0 & 1 & 0 & 0 \end{matrix}$$

$$
(8)\qquad
\begin{matrix}
0 & 0 & 0 & -1 & 0 & 0 & 0 \\
0 & 0 & 0 & 5 & 0 & 0 & 0 \\
0 & 0 & 0 & -10 & 0 & 0 & 0 \\
0 & 0 & 0 & 10 & 0 & 0 & 0 \\
0 & 0 & 0 & -5 & 0 & 0 & 0 \\
0 & 0 & 0 & 1 & 0 & 0 & 0 \\
0 & 0 & 0 & 0 & 0 & 0 & 0
\end{matrix}
$$

$$
(9)\qquad
\begin{matrix}
0 & 0 & 0 & 1 & 0 & 0 & 0 \\
0 & 0 & 0 & -6 & 0 & 0 & 0 \\
0 & 0 & 0 & 15 & 0 & 0 & 0 \\
0 & 0 & 0 & -20 & 0 & 0 & 0 \\
0 & 0 & 0 & 15 & 0 & 0 & 0 \\
0 & 0 & 0 & -6 & 0 & 0 & 0 \\
0 & 0 & 0 & 1 & 0 & 0 & 0
\end{matrix}
$$

The masks for 1<u>st</u> through 6<u>th</u> differences in the E-W direction are:

$$
(10)\qquad
\begin{matrix}
0 & 0 & 0 \\
-1 & 1 & 0 \\
0 & 0 & 0
\end{matrix}
$$

$$
(11)\qquad
\begin{matrix}
0 & 0 & 0 \\
1 & -2 & 1 \\
0 & 0 & 0
\end{matrix}
$$

$$
(12)\qquad
\begin{matrix}
0 & 0 & 0 & 0 & 0 \\
0 & 0 & 0 & 0 & 0 \\
-1 & 3 & -3 & 1 & 0 \\
0 & 0 & 0 & 0 & 0 \\
0 & 0 & 0 & 0 & 0
\end{matrix}
$$

$$
(13)\qquad
\begin{matrix}
0 & 0 & 0 & 0 & 0 \\
0 & 0 & 0 & 0 & 0 \\
1 & -4 & 6 & -4 & 1 \\
0 & 0 & 0 & 0 & 0 \\
0 & 0 & 0 & 0 & 0
\end{matrix}
$$

$$
(14)\qquad
\begin{matrix}
0 & 0 & 0 & 0 & 0 & 0 & 0 \\
0 & 0 & 0 & 0 & 0 & 0 & 0 \\
0 & 0 & 0 & 0 & 0 & 0 & 0 \\
-1 & 5 & -10 & 10 & -5 & 1 & 0 \\
0 & 0 & 0 & 0 & 0 & 0 & 0 \\
0 & 0 & 0 & 0 & 0 & 0 & 0 \\
0 & 0 & 0 & 0 & 0 & 0 & 0
\end{matrix}
$$

$$
(15)\qquad
\begin{matrix}
0 & 0 & 0 & 0 & 0 & 0 & 0 \\
0 & 0 & 0 & 0 & 0 & 0 & 0 \\
0 & 0 & 0 & 0 & 0 & 0 & 0 \\
1 & -6 & 15 & -20 & 15 & -6 & 1 \\
0 & 0 & 0 & 0 & 0 & 0 & 0 \\
0 & 0 & 0 & 0 & 0 & 0 & 0 \\
0 & 0 & 0 & 0 & 0 & 0 & 0
\end{matrix}
$$

The masks for $1\underline{st}$ through $6\underline{th}$ differences in the NW-SE direction are:

$$(16)\quad \begin{matrix} -1 & 0 & 0 \\ 0 & 1 & 0 \\ 0 & 0 & 0 \end{matrix}$$

$$(17)\quad \begin{matrix} 1 & 0 & 0 \\ 0 & -2 & 0 \\ 0 & 0 & 1 \end{matrix}$$

$$(18)\quad \begin{matrix} -1 & 0 & 0 & 0 & 0 \\ 0 & 3 & 0 & 0 & 0 \\ 0 & 0 & -3 & 0 & 0 \\ 0 & 0 & 0 & 1 & 0 \\ 0 & 0 & 0 & 0 & 0 \end{matrix}$$

$$(19)\quad \begin{matrix} 1 & 0 & 0 & 0 & 0 \\ 0 & -4 & 0 & 0 & 0 \\ 0 & 0 & 6 & 0 & 0 \\ 0 & 0 & 0 & -4 & 0 \\ 0 & 0 & 0 & 0 & 1 \end{matrix}$$

$$(20)\quad \begin{matrix} -1 & 0 & 0 & 0 & 0 & 0 & 0 \\ 0 & 5 & 0 & 0 & 0 & 0 & 0 \\ 0 & 0 & -10 & 0 & 0 & 0 & 0 \\ 0 & 0 & 0 & 10 & 0 & 0 & 0 \\ 0 & 0 & 0 & 0 & -5 & 0 & 0 \\ 0 & 0 & 0 & 0 & 0 & 1 & 0 \\ 0 & 0 & 0 & 0 & 0 & 0 & 0 \end{matrix}$$

$$(21)\quad \begin{matrix} 1 & 0 & 0 & 0 & 0 & 0 & 0 \\ 0 & -6 & 0 & 0 & 0 & 0 & 0 \\ 0 & 0 & 15 & 0 & 0 & 0 & 0 \\ 0 & 0 & 0 & -20 & 0 & 0 & 0 \\ 0 & 0 & 0 & 0 & 15 & 0 & 0 \\ 0 & 0 & 0 & 0 & 0 & -6 & 0 \\ 0 & 0 & 0 & 0 & 0 & 0 & 1 \end{matrix}$$

The masks for $1\underline{st}$ through $6\underline{th}$ differences in the SW-NE direction are:

$$(22)\quad \begin{matrix} 0 & 0 & 0 \\ 0 & 1 & 0 \\ -1 & 0 & 0 \end{matrix}$$

$$(23)\quad \begin{matrix} 0 & 0 & 1 \\ 0 & -2 & 0 \\ 1 & 0 & 0 \end{matrix}$$

$$
(24)\qquad \begin{matrix} 0 & 0 & 0 & 0 & 0 \\ 0 & 0 & 0 & 1 & 0 \\ 0 & 0 & -3 & 0 & 0 \\ 0 & 3 & 0 & 0 & 0 \\ -1 & 0 & 0 & 0 & 0 \end{matrix}
$$

$$
(25)\qquad \begin{matrix} 0 & 0 & 0 & 0 & 1 \\ 0 & 0 & 0 & -4 & 0 \\ 0 & 0 & 6 & 0 & 0 \\ 0 & -4 & 0 & 0 & 0 \\ 1 & 0 & 0 & 0 & 0 \end{matrix}
$$

$$
(26)\qquad \begin{matrix} 0 & 0 & 0 & 0 & 0 & 0 & 0 \\ 0 & 0 & 0 & 0 & 0 & 1 & 0 \\ 0 & 0 & 0 & 0 & -5 & 0 & 0 \\ 0 & 0 & 0 & 10 & 0 & 0 & 0 \\ 0 & 0 & -10 & 0 & 0 & 0 & 0 \\ 0 & 5 & 0 & 0 & 0 & 0 & 0 \\ -1 & 0 & 0 & 0 & 0 & 0 & 0 \end{matrix}
$$

$$
(27)\qquad \begin{matrix} 0 & 0 & 0 & 0 & 0 & 0 & 1 \\ 0 & 0 & 0 & 0 & 0 & -6 & 0 \\ 0 & 0 & 0 & 0 & 15 & 0 & 0 \\ 0 & 0 & 0 & -20 & 0 & 0 & 0 \\ 0 & 0 & 15 & 0 & 0 & 0 & 0 \\ 0 & -6 & 0 & 0 & 0 & 0 & 0 \\ 1 & 0 & 0 & 0 & 0 & 0 & 0 \end{matrix}
$$

Appendix E COLCR TRANSFORMATION FOR CRT DISPLAYS

Color displays such as CRT devices use the additive color principle to generate their spectra of colors. Red, green and blue shades are the usual primaries in color CRT displays. When three types of data are to be displayed, the most common (and easiest) process is to allow one data set to control the red, one the green and one the blue. This process is valid for reconstructing a color scene from its red, green and blue components, but generally it is not valid if the objective is to maximize the amount of information perceived from each of the three data sets by the human observer. This is due to the nature of the eye and the processing of information by the visual system [1].

What is needed to maximize perception is a set of parameters which specify a given color and which are nearly independent of each other. Without going into the details it can be argued that intensity, hue and saturation are parameters which satisfy these conditions.

Intensity is the apparent brightness of a display. Hue is the predominant "color". Saturation measures how much a hue is "diluted" by white. On the C.I.E.* chromaticity diagram, which maps color perception, saturation and hue can be approximately represented by a polar coordinate system. Saturation is represented by the radial distance of a color from white which lies at the origin of the coordinate system. Hue is represented by an angular measure around the origin from an arbitrary reference hue. Intensity would be represented by a vector perpendicular to the hue - saturation plane. With these three parameters any color can be uniquely defined. This method of defining color is called the IHS (intensity, hue, saturation) representation. It should be noted that this representation defines a cylindrical coordinate system which will be used later.

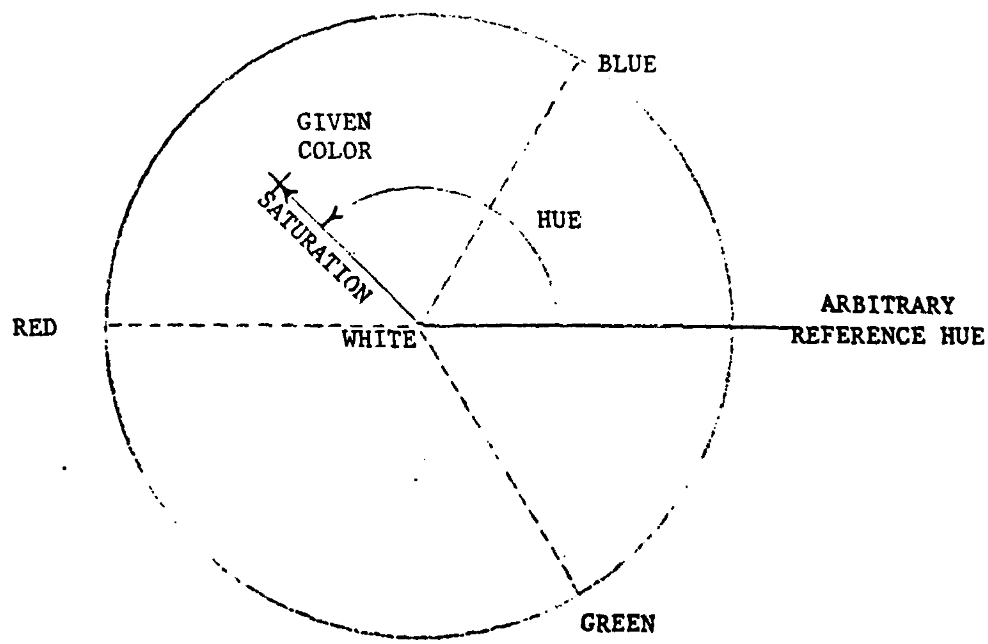

Figure E.1 HUE-SATURATION PLANE

* Commission Internationale de L'Eclairage

The choice of three primaries, such as those in a CRT display, defines a triangle in the hue-saturation plane. Any hue or saturation can be achieved within the triangle by varying the relative amounts of each primary. Unfortunately, colors outside of the triangle cannot be achieved unless new primaries are chosen. Intensity on the display can be varied by changing the sum of the amounts of the three primaries. (This defines intensity and is based on the work done by Faugeras. [1]) Since the maximum intensity of each primary is limited in a CRT display, the maximum intensity of any mixture is also limited.

Both the RGB and IHS color representations can uniquely and completely specify any color, therefore, there must exist a transformation that will take the parameters of a color in RGB and give the parameters in IHS and vice versa. This transformation is now derived with the restrictions of CRT displays in mind and with some simplifying assumptions.

Negative values are not possible for the primary values, so colors are restricted to be in the positive octant. Since the intensity is represented as being proportional to the sum of the three primary components, an intensity coordinate can be defined as a vector starting at the origin and in a direction equidistant from each RGB axis. This vector is perpendicular to any plane of constant intensity defined by

$$R + B + G = \text{constant}$$

With the intensity vector defined we can relate the cylindrical coordinate system of IHS space to the rectangular coordinate system of RGB space. The transformation is from cylindrical to rectangular coordinates with a rotation.

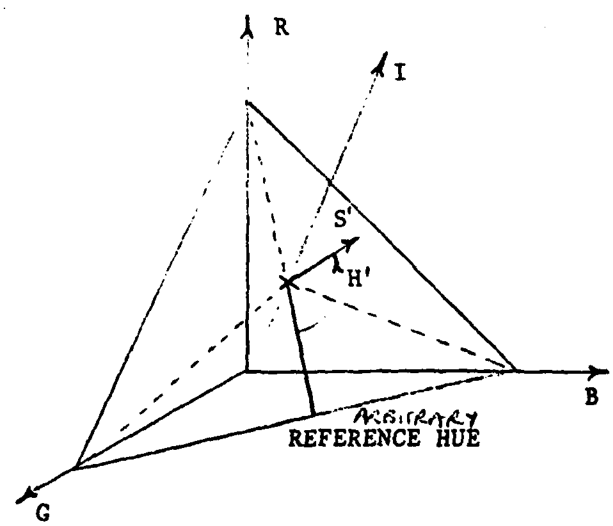

Figure E.2 GEOMETRY RELATING IHS TO RGB

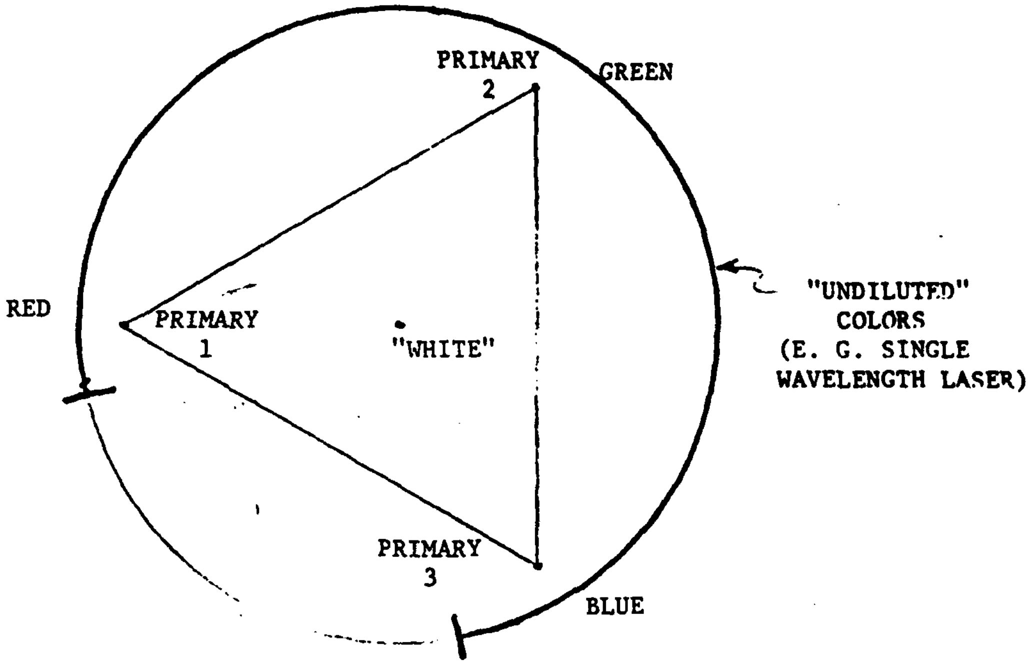

Figure E.3 RELATION OF PRIMARIES TO CHROMATICITY

For derivation purposes the three RGB primaries are assumed to form an equilateral triangle in the hue - saturation plane. "White" contains an equal amount of each of the primaries. In RGB space each of the primaries is assumed to lie along the axis of a three dimensional rectangular coordinate system.

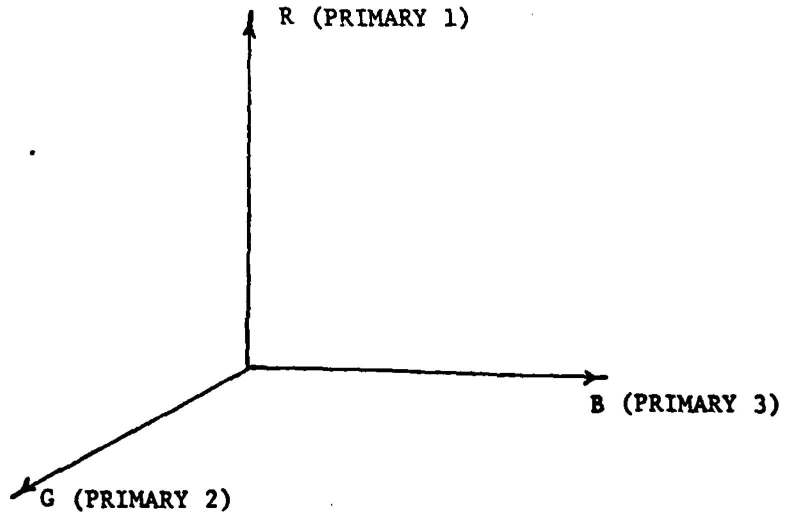

Figure E.4 COORDINATE SYSTEM DEFINED BY PRIMARIES

For the rotation to line up the R axis with the I axis.

$$\begin{bmatrix} R \\ G \\ B \end{bmatrix} = \frac{1}{\sqrt{3}} \begin{bmatrix} 1 & -1 & -1 \\ 1 & \frac{1+\sqrt{3}}{2} & \frac{1-\sqrt{3}}{2} \\ 1 & \frac{1-\sqrt{3}}{2} & \frac{1+\sqrt{3}}{2} \end{bmatrix} \begin{bmatrix} R' \\ G' \\ B' \end{bmatrix}$$

For the transformation from cylindrical to rectangular coordinates.

$$R' = I \qquad -\infty<I<\infty$$

$$G' = S' \cos H' \qquad 0<S'<\infty$$

$$B' = S' \sin H' \qquad 0\leq H'<2\pi$$

Combining the two transformations

$$R = \frac{1}{\sqrt{3}} (I-S'(\cos H' + \sin H')) \qquad -\infty<I<\infty$$

$$G = \frac{1}{\sqrt{3}} (I+S'(\frac{1+\sqrt{3}}{2} \cos H' + \frac{1-\sqrt{3}}{2} \sin H')) \qquad 0<S'<\infty$$

$$B = \frac{1}{\sqrt{3}} (I+S'(\frac{1-\sqrt{3}}{2} \cos H' + \frac{1+\sqrt{3}}{2} \sin H')) \qquad 0\leq H'<2\pi$$

For completeness, the inverse transformation is

$$I = \frac{R + G + B}{\sqrt{3}}$$

$$S'^2 = \frac{R^2 - RB - RG + 2BG - B^2/2 - G^2/2}{3}$$

$$\tan H' = \frac{(1-\sqrt{3})G + (1+\sqrt{3})B - 2R}{(1+\sqrt{3})G + (1-\sqrt{3})B - 2R}$$

$$-\infty<R<\infty$$

$$-\infty<G<\infty$$

$$-\infty<B<\infty$$

So far, the derivation has strictly been a mathematical coordinate transformation. The next step is to account for the physical constraints of the color display on the RGB values, more specifically,

$$0 \le R, B, G \le 1$$

In this case

$$0 \le I \le 1/\sqrt{3}$$

and

$$0 \le S' \le \frac{\sqrt{2}\,I}{\sqrt{3}}$$

The saturation must be proportional to the intensity for the relative amounts of red, green and blue to remain constant. To visualize the reachable colors with this transformation I is set to ~~its maximum~~ a constant and the hue - saturation plane is examined.

[redacted]

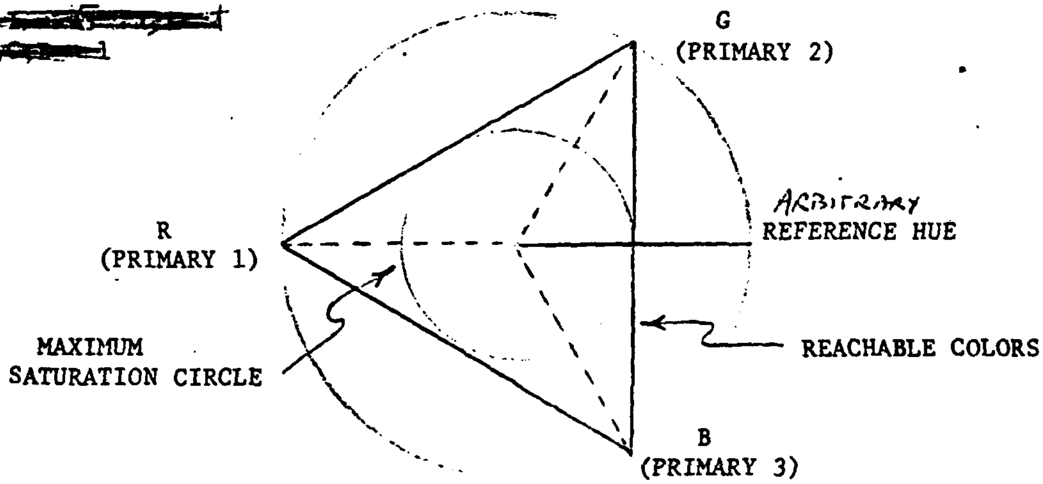

Figure E.5 TRANSFORMATION LIMITATION ON ACHIEVABLE COLORS

The triangle defines the total spectrum of achievable colors with the chosen primaries. The inner circle defines those colors achievable with the above transformation.

All the colors inside the triangle can be reached if slight adjustments are made to the hue and saturation. First we change the reference hue so that it corresponds to pure red

$$H' = H + 3\pi/4$$

then we alter the saturation for different values of hue

$$S' = \frac{\sqrt{3}S}{2\sin(\frac{5\pi}{6}-H')} \qquad 0 \le H' < \frac{2\pi}{3}$$

$$= \frac{\sqrt{3}S}{2\sin(\frac{3\pi}{2}-H')} \qquad \frac{2\pi}{3} < H' < \frac{4\pi}{3}$$

$$= \frac{\sqrt{3}S}{2\sin(\frac{13\pi}{6}-H')} \qquad \frac{4\pi}{3} < H' < 2\pi$$

These values of H' and S' can be used in the transformation equations given previously.

This derivation seems to yield good results on actual displays but several areas of study could still be pursued:

1) A more precise approach to using Faugeras' eye model.

2) In general three primaries do not form an equilateral triangle on the C.I.E. chromaticity diagram.

3) Hue and saturation do not appear as polar coordinates on the C.I.E. diagram.

Reference

[1] O. D. Faugeras, "Digital Color Image Processing," IEEE Transactions on Acoustics, Speech, and Signal Processing, vol. ASSP-27 pp. 380-393, August 1979.

DATE
ILMED
8